

A strong negative correlation between radio loudness R_{UV} and optical-to-X-ray spectral index α_{ox} in low-luminosity AGNs

Shuang-Liang Li* and Fu-Guo Xie*

Key Laboratory for Research in Galaxies and Cosmology, Shanghai Astronomical Observatory, Chinese Academy of Sciences, 80 Nandan Road, 200030 Shanghai, China

6 October 2018

ABSTRACT

It has been argued for years that the accretion mode changes from bright active galactic nuclei (AGNs) to low-luminosity AGNs (LLAGNs) at a rough dividing point of bolometric Eddington ratio $\lambda \sim 10^{-2}$. In this work, we strengthen this scenario through investigation of the relationship between the radio loudness R_{UV} and the optical-to-X-ray spectral index α_{ox} in LLAGNs with $10^{-6} \lesssim \lambda \lesssim 10^{-3}$. We compile from literature a sample of 32 LLAGNs, consisting 18 LINERs and 14 low Eddington ratio Seyfert galaxies, and observe a strong negative $R_{UV}-\alpha_{ox}$ relationship, with large scatter in both R_{UV} and α_{ox} . We further demonstrate that this negative correlation, and the additional two negative relationships reported in literature ($R_{UV}-\lambda$ and $\alpha_{ox}-\lambda$ correlations), can be understood consistently and comprehensively under the truncated accretion–jet model, the model that has been applied successfully applied to LLAGNs. We argue that the scatter in the observations are (mainly) due to the spread in the viscosity parameter α of a hot accretion flow, a parameter that potentially can serve as a diagnose of the strength and/or configuration of magnetic fields in accretion flows.

Key words: accretion, accretion discs – black hole physics – galaxies: active – galaxies: Seyfert

1 INTRODUCTION

It has been known for years that statistically low-luminosity active galactic nuclei (AGNs), whose bolometric Eddington ratios (defined as the bolometric luminosity L_{bol} in Eddington unit, i.e. $\lambda \equiv L_{bol}/L_{Edd}$, where $L_{Edd} \equiv 1.3 \times 10^{46} \text{erg s}^{-1} (M_{BH}/10^8 M_{\odot})$ is the Eddington luminosity and M_{BH} is the black hole mass) are lower than $\sim 1 - 2 \times 10^{-2}$, are distinctive in various aspects to those bright AGNs (see Ho 2008 for a review). At first, the big blue bump disappears in LLAGNs (Shang et al. 2005; Ho 2009). Secondly, Xu (2011) and Sobolewska et al. (2011) found that the optical-to-X-ray spectral index α_{ox} (flux $F_{\nu} \propto \nu^{-\alpha_{ox}}$, or equivalently, $\alpha_{ox} = \log [L_{\nu}(2500 \text{ \AA})/L_{\nu}(2 \text{ keV})] / \log [\nu(2500 \text{ \AA})/\nu(2 \text{ keV})] = 0.384 \log [L_{\nu}(2500 \text{ \AA})/L_{\nu}(2 \text{ keV})]$.) correlates negatively with the bolometric Eddington ratio λ in LLAGNs, but positively in bright AGNs. Thirdly, Gu & Cao (2009) reported an anti-correlation between the hard 2–10 keV X-ray photon index Γ and the Eddington ratio λ in LLAGNs, in contrast with the positive correlation found in bright AGNs (see also Yang et al. 2015). Fourthly, opposite correlations between the radio loudness and the luminosity ratio are also observed in LLAGNs and bright AGNs (Greene, Ho & Ulvestad 2006). Compared with black hole

(BH) X-ray binaries (BHBs), all the above observations hint (see e.g., Greene, Ho & Ulvestad 2006; Ho 2008; Sobolewska et al. 2011; Yang et al. 2015) that LLAGNs and bright AGNs are likely analogy to BHBs in their hard and soft states (see Belloni 2010 for definitions of states in BHBs), respectively (but also see Done 2014).

From theoretical point of view, the accretion mode is different between LLAGNs (and BHBs in hard state) and bright AGNs (and BHBs in soft state). The BHBs in their soft state can be well described by an optically thick, geometrically thin accretion disc (Shakura & Sunyaev 1973; the so-called Shakura-Sunyaev disc, SSD hereafter.), which emits thermal radiation. This thermal emission will appear in X-rays for BHBs in soft state. The SSD around supermassive BHs will be much cooler than that around stellar BHs (the case of BHBs), and they will emit in optical-to-ultraviolet (UV) bands. This will naturally explain the big blue bump commonly observed in bright AGNs. Additional observations also require a weak hot corona component, which contributes to the X-ray emissions. The BHBs in their hard state and the LLAGNs, on the other hand, will be better described by the truncated accretion–jet model (Esin et al. 1997; Lasota et al. 1996; Yuan et al. 2003; Wu et al. 2007. For reviews see Done et al. 2007; Ho 2008; Yuan & Narayan 2014). In this model, the cold SSD is truncated at certain radius, within which it is replaced by a hot accretion flow. Besides, there is a relativistic jet near

* E-mails: lisl@shao.ac.cn (S.L.L.); fgxie@shao.ac.cn (F.G.X.)

the BH. Generally the hot accretion flow is an update version of the conventional advection-dominated accretion flow (ADAF; Narayan & Yi 1994, 1995; Blandford & Begelman 1999; Yuan et al. 2012, 2015; Bu et al. 2013, 2016; Sadowski et al. 2015), and it is usually optically thin but geometrically thick (for review see Yuan & Narayan 2014).

Given the above simple theoretical interpretation, further investigations are required, in order to understand observations in detail. For example, apart from the global trends observed, large dispersion is also witnessed in both the Γ - λ correlation (e.g., Gu & Cao 2009; Yang et al. 2015) and the α_{ox} - λ correlation (e.g., Xu 2011; Sobolewska et al. 2011). Obviously these large scatter indicates that, besides the accretion rate \dot{M} which controls the luminosities in different wavebands, additional parameters/factors awaiting to be identified should also play certain roles. One possible factor is the difference in the viscosity parameter α of the hot accretion flow among different systems. Under a hot accretion flow model, systems with larger α can transport angular momentum more easily. Consequently, for a given accretion rate, these high- α systems will have higher infalling velocity and lower gas density, which results in lower broadband emission with larger α_{ox} (Manmoto et al. 1997; Esin et al. 1997, and Section 4 for more discussions). Interestingly, based on local shearing-box magnetohydrodynamic (MHD) simulations of hot accretion flows, the “effective” viscosity parameter indeed can vary significantly, for a moderate change in the net magnetic flux and/or magnetic field configuration carried by the accreted material (e.g., Hawley et al. 1995; Backman et al. 2008; Bai & Stone 2013; Salvesen et al. 2016). Besides, the viscosity parameter of its hot accretion component in AGN NGC 7213 can be well-constrained based on observations of a hybrid radio/X-ray correlation together with a V-shaped X-ray index/luminosity correlation (Xie et al. 2016), i.e. $\alpha \approx 0.01$, a value considerably smaller compared to the typical value of hot accretion flows ($\alpha \sim 0.1 - 0.3$, see e.g., Yuan et al. 2003; Wu et al. 2007; Yu et al. 2011).

With the motivation to reveal the possible impact of viscosity parameter α (or more aggressively, the strength and/or configuration of magnetic field) of hot accretion flows, we in this work only consider quantities that relate to relative luminosities (i.e. Eddington ratios) instead of absolute ones, hoping to (partially) eliminate the impact of black hole mass. In practice, we focus on the optical-to-X-ray spectral index α_{ox} and the radio-loudness R_{UV} in LLAGNs. Here parameter radio-loudness R_{UV} is defined as the ratio between the radio luminosity (spectral, at 5 GHz, $L_{\text{R}} = L_{\nu}(5 \text{ GHz})$) and UV luminosity (spectral, at 2500 Å, $L_{\text{UV}} = L_{\nu}(2500 \text{ Å})$), i.e. $R_{\text{UV}} = L_{\text{R}}/L_{\text{UV}}$. The sample compilation is shown in Section 2. Since we target at hot accretion (e.g., ADAF) dominated systems, we thus limit ourselves to systems whose Eddington ratio $\lambda \lesssim 10^{-3}$, an order of magnitude lower than the typical critical luminosity ($\lambda_{\text{crit}} \sim 10^{-2}$) between bright AGNs and LLAGNs. We further exclude from our sample several faint sources whose X-rays may be of jet origin instead of hot accretion flow origin. Our final LLAGN sample includes 32 sources, among which 14 are low luminosity (in the sense of Eddington ratio λ) Seyfert galaxies and 18 are low-ionization nuclear emission-line region (LINER) galaxies. The Eddington ratio is in the range $10^{-6} \lesssim \lambda \lesssim 10^{-3}$. The results are shown in Section 3, where we report a strong negative correlation between R_{UV} and α_{ox} in LLAGNs, independent of the luminosities. Interestingly, such correlation seems to be invisible based on a small sample of bright AGNs (See Section 3.2 for details.). Additional correlations, e.g. $R_{\text{UV}}-\lambda$ and $\alpha_{\text{ox}}-\lambda$ relationships are also reported. We then in Sec-

tion 4 provide a comprehensive interpretation on the results (both the correlation and the scatter), based on the truncated accretion-jet model. Finally, Section 5 is devoted to a brief summary.

2 THE LLAGN SAMPLE WITH EDDINGTON RATIO

$$10^{-6} \lesssim \lambda \lesssim 10^{-3}$$

We gather from literature a sample of LLAGNs, which consist of both LINERs and low- λ Seyfert galaxies. Firstly, we collect the nuclear emission of 16 low-luminosity Seyfert galaxies from Xu (2011). All the objects in Xu (2011) were gathered by Gu & Cao (2009) from the Palomar sample (Ho et al. 1997a; Ho 2008) and the multi-wavelength catalog of LINERs (Carrillo et al. 1999), where all the sources have *Chandra* and/or *XMM-Newton* observations. Xu (2011) further excluded six LINERs who lack estimation in UV luminosities. The optical luminosity at 2500 Å is derived from the absolute B magnitude mainly observed by high-spatial-resolution *Hubble Space Telescope* (HST, Ho et al. 1997a,b), with the assumption that the optical-UV spectral index is $\alpha_o = -1$, a typical value for the optical featureless continuum of Seyfert 1 nuclei (Ward et al. 1987), cf. Xu (2011) for details. For the core emission of LINERs, we gather from Maoz (2007) and Xu (2011), which includes respectively, 13 and 20 sources. The data compilation of LINERs is the same to that of Seyferts in Xu (2011). The sample of Maoz (2007) are from Maoz et al. (2005), where four objects are excluded for different reasons (see Maoz 2007 for details). All the objects in Maoz et al. (2005) are optically classified as LINERs by Ho et al. (1997a), and they are selected provided their UV is observed by high-resolution HST and their nuclei X-ray emission is from *Chandra* (or *XMM-Newton*). Considering the duplicates in the two works, there are 27 LINERs left in total. We note that there are other LINER samples in literature, e.g., Younes et al. (2011), Hernández-García et al. (2013), and Connolly et al. (2016), and all these samples are also selected from Ho et al. (1997a,b) and/or Carrillo et al. (1999). Consequently, except for several sources that lack constraints in X-ray photon index Γ , most of them overlap with the samples of Maoz (2007) and Xu (2011).

Additionally, there are faint LLAGNs whose X-rays may be dominated by emission from relativistic jets rather than hot accretion flows (e.g., Yuan et al. 2009; Nemmen et al. 2010, 2014; Xie & Yuan 2017), and these sources are not justified for our scientific motivation (to investigate the properties of a hot accretion flow itself), thus should be excluded from our sample. From theoretical point of view, it is because, as the accretion rate reduces, the relative importance of jet emission increases (Yuan & Cui 2005). Below a certain critical luminosity (statistically the critical luminosity is $L_{\text{X}}(2 - 10 \text{ keV}) \sim 10^{-6} L_{\text{Edd}}$; Yuan & Cui 2005; Yuan et al. 2009; Xie & Yuan 2017), the X-ray emission from jets will exceed that of hot accretion flows. Six sources (NGC3031, NGC3998, NGC4374, NGC4486, NCG4552, NGC4594) are excluded from our sample, as they have confirmation of the jet origin in X-rays from multi-waveband spectral modelling (Wu et al. 2007; Yuan et al. 2009; Yu et al. 2011; Nemmen et al. 2014). Besides, The other five sources (NGC3941, NGC3226, NGC3169, NGC6500, and NGC7130) are also excluded from our sample, for the reason that their X-ray spectra are relatively soft, with photon index $\Gamma > 2$ (Maoz 2007; Gu & Cao 2009), which is suggestive of a jet origin in X-rays considering their faintness in X-rays (Cao & Wang 2014; Nemmen et al. 2014; Yang et al. 2015).

As listed in Table 1, our final LLAGN sample includes 14 low- λ Seyfert galaxies and 18 LINERs. Sources with superscript

Table 1. The sample of LLAGNs with $10^{-6} \lesssim \lambda \lesssim 10^{-3}$.

Name (1)	$\log M_{BH}/M_{\odot}$ (2)	$\log L_R$ (3)	$\log L_{UV}$ (4)	$\log L_X$ (5)	$\log \lambda$ (6)	$\log R_{UV}$ (7)	$\log R_X$ (8)	α_{ox} (9)
<i>Seyfert galaxies</i>								
NGC 2639 ^(a)	8.02	29.52	<24.18	22.80	-3.82	>5.34	6.72	<0.53
NGC 4138 ^(a)	7.75	28.98	<23.94	23.21	-3.08	>5.04	5.77	<0.28
NGC 4168 ^(a)	7.95	27.88	<22.97	21.98	-4.70	>4.91	5.90	<0.38
NGC 4258 ^(a)	7.61	26.25	<23.36	22.75	-3.37	>2.89	3.5	<0.24
NGC 4565 ^(a)	7.70	27.22	24.79	21.47	-4.89	2.43	5.75	1.28
NGC 4579 ^(a)	7.78	28.50	25.55	23.10	-3.37	2.95	5.40	0.94
NGC 4639 ^(a)	6.85	27.65*	24.19	22.26	-3.25	3.46	5.39	0.74
NGC 2685 ^(a)	7.15	26.07	23.96	21.42	-3.82	2.11	4.65	0.97
NGC 3147 ^(a)	8.79	28.23	25.12	23.96	-3.52	3.11	4.27	0.45
NGC 3486 ^(a)	6.14	28.13	23.06	20.53	-3.89	5.07	7.60	0.97
NGC 4477 ^(a)	7.92	27.55*	24.29	21.72	-4.89	3.26	5.83	0.99
NGC 4501 ^(a)	7.90	27.60	24.79	21.51	-4.92	2.81	6.09	1.26
NGC 4698 ^(a)	7.84	27.09*	23.74	21.27	-5.30	3.35	5.82	0.95
NGC 4725 ^(a)	7.49	28.12*	23.53	20.96	-5.22	4.59	7.16	0.99
<i>LINERs</i>								
NGC 266 ^(a)	7.90	28.22	25.50	22.76	-3.64	2.72	5.46	1.05
NGC 0315 ^(a)	9.24	30.47	25.55	23.56	-4.22	4.92	6.91	0.77
NGC 2681 ^(a)	7.20	27.48*	24.10	20.95	-4.88	3.88	6.53	1.21
NGC 3718 ^(a)	7.97	27.34	23.83	21.97	-4.53	3.51	5.37	0.71
NGC 4143 ^(a)	8.31	28.31	24.67	22.03	-4.89	3.64	6.28	1.02
NGC 4278 ^(a)	9.20	28.54	24.72	21.94	-5.86	3.82	6.60	1.07
NGC 4261 ^(a)	8.94	29.76	24.81	22.73	-4.41	4.95	7.03	0.80
NGC 4457 ^(a)	7.00	27.71*	25.00	20.99	-4.63	2.71	6.72	1.54
NGC 4494 ^(a)	7.60	26.83*	23.88	21.04	-5.22	2.95	5.79	1.09
NGC 4548 ^(a)	7.51	26.92*	23.43	21.79	-4.34	3.49	5.13	0.63
NGC 4736 ^(a)	7.42	26.40	23.25	20.76	-5.39	3.15	5.64	0.96
NGC 5746 ^(a)	7.49	29.02*	23.55	21.88	-4.04	5.47	7.14	0.64
NGC 6240 ^(a)	9.11	29.73	27.73	23.77	-3.69	2.00	5.96	1.52
NGC 404 ^(b)	5.30	<24.74	24.67	19.46	-4.84	<0.08	<5.28	2.00
NGC 1052 ^(b)	8.10	29.98	25.16	22.86	-4.12	4.81	7.12	0.89
NGC 3386 ^(b)	7.40	<26.01	24.87	21.38	-5.02	<1.14	<4.63	1.34
NGC 3642 ^(b)	7.10	<26.65	25.70	22.61	-3.49	<0.96	<4.04	1.19
NGC 4203 ^(b)	7.00	27.55	25.56	22.67	-3.33	1.79	4.68	1.11

Notes: Col.(1): Source name. Here the superscripts ^(a) and ^(b) represent sources that are taken from Xu (2011) and Maoz (2007), respectively. Col.(2): Black hole mass. Col.(3): radio spectral luminosity at 5 GHz, L_R , in unit of $\text{erg s}^{-1} \text{Hz}^{-1}$. Col.(4): UV spectral luminosity at 2500 Å, L_{UV} , in unit of $\text{erg s}^{-1} \text{Hz}^{-1}$. Col.(5): X-ray spectral luminosity at 2 keV, L_X , in unit of $\text{erg s}^{-1} \text{Hz}^{-1}$. Col.(6): Eddington ratio, $\lambda = L_{bol}/L_{Edd}$. Col.(7): Radio loudness $R_{UV} \equiv L_R/L_{UV}$. Col.(8): Radio loudness defined as, $R_X = L_R/L_X$. Col.(9): optical-to-X-ray spectral index $\alpha_{ox} \equiv 0.384 \log [L_{UV}/L_X]$.

*: For sources labelled with *, their radio flux at 5 GHz are derived based on observations at neighbouring frequencies.

Table 2. The sample of bright AGNs with $\lambda > 10^{-2}$.

Name (1)	$\log M_{BH}/M_{\odot}$ (2)	$\log L_R$ (3)	$\log L_{UV}$ (4)	$\log L_X$ (5)	$\log \lambda$ (6)	$\log R_{UV}$ (7)	$\log R_X$ (8)	α_{ox} (9)
<i>Seyfert galaxies</i>								
NGC 3516 ^(a)	7.36	27.55	27.14	24.14	-1.70	0.41	3.41	1.15
NGC 4051 ^(a)	6.11	27.26	25.72	23.16	-1.42	1.54	4.10	0.98
NGC 4151 ^(a)	7.18	28.64	27.56	24.31	-1.33	1.08	4.33	1.25
NGC 4388 ^(a)	6.80	28.81	26.14	23.72	-1.70	2.67	5.09	0.93
NGC 4395 ^(a)	5.04	25.59	24.16	21.65	-1.85	1.43	3.94	0.96
NGC 5273 ^(a)	6.51	26.86	25.53	23.27	-1.77	1.33	3.59	0.87
NGC 5548 ^(a)	8.03	28.87	27.16	25.25	-1.40	1.71	3.62	0.74

Notes: Col.(1)-(9) are the same as those in Table 1.

^(a) in Table 1 are gathered from Xu (2011). For these sources, Cols.(1), (2), (4), (5), (6) and (9) are directly taken from Xu (2011). We additionally gather its nuclear radio luminosity at 5 GHz from NED,¹ as shown in Col. (3). For sources without radio observations at 5 GHz (labelled with superscript *), we derive its spectral radio luminosity at 5 GHz based on observations at neighbouring frequencies, with the spectral index in radio wavebands assumed to be $\alpha_r \approx 0$. This choice of α_r comes from the fact that the radio spectra of LLAGNs tend to be flat or even slightly reverted (see, e.g., Ulvestad & Ho 2001; Ho 2008), a signature of self-absorbed synchrotron emission from conical relativistic “continuous” jet (Blandford & Königl 1979). Such derivation of L_R should not introduce large scatter to the correlations reported later in this work, since we usually have $-0.3 < \alpha_r < 0.3$ for LLAGNs (Ulvestad & Ho 2001; Ho 2008), and the adopted frequency is close to 5 GHz. With L_R , we subsequently can calculate the radio loudnesses R_{UV} and R_X (here we define $R_X = L_R/L_X$, following Ho 2008.), respectively, which are shown in Cols.(7) & (8).

For sources with superscript ^(b) in Table 1, all data except Col.(6) and Col.(8) are adopted from Maoz (2007) directly. The Eddington ratio in Col. (6) is estimated based on its 2-10 keV X-ray luminosity $L_X(2 - 10 \text{ keV})$, i.e. we assume the bolometric luminosity $L_{\text{bol}} \approx 30 L_X(2 - 10 \text{ keV})$, the same as that in Xu (2011). Note that another correction $L_{\text{bol}} \approx 16 L_X(2 - 10 \text{ keV})$, which is approximately a factor of ~ 2 lower than our choice, is also widely adopted in literature (see e.g., Ho 2008). Since our results are insensitive to the exact bolometric luminosity of each source, we omit further discussions on the two corrections below.

3 RESULTS AND DISCUSSIONS

3.1 basic properties of the LLAGN sample

Before we investigate the relationship between R_{UV} and α_{ox} , we first show in Fig. 1 the general properties of our sample. We divide our sample into three luminosity regimes, i.e. $-6 < \log \lambda < -5$ (blue triangles in all the plots), $-5 < \log \lambda < -4$ (green circles) and $-4 < \log \lambda < -3$ (red squares).

From the top panel of Fig. 1, a liner fit (in logarithmic space) between R_{UV} and λ reads,

$$\log R_{UV} = (0.04 \pm 0.33) \log \lambda + 3.51 \pm 1.44, \quad (1)$$

where the confidence level of rejecting a null hypothesis is 9.4 %, based on Pearson test. We note that based on larger samples that have sufficiently large dynamical range in λ (especially the bright end), we will normally observe a negative R_{UV} - λ correlation (Maoz 2007; Sikora et al. 2007). Since the null (or weak positive) R_{UV} - λ correlation observed in our work suffers large uncertainties in the correlation slope, we will rely on those previous works later for the theoretical interpretation.

The relationship between R_X and λ , on the other hand, is much stronger (cf. the middle panel of Fig. 1), i.e. a liner fit in logarithmic space gives,

$$\log R_X = (-0.46 \pm 0.23) \log \lambda + 3.83 \pm 1.00, \quad (2)$$

whose confidence level is 94.7 %. This negative R_X - λ correlation had been reported in numerous works (cf., Ho 2008 and references

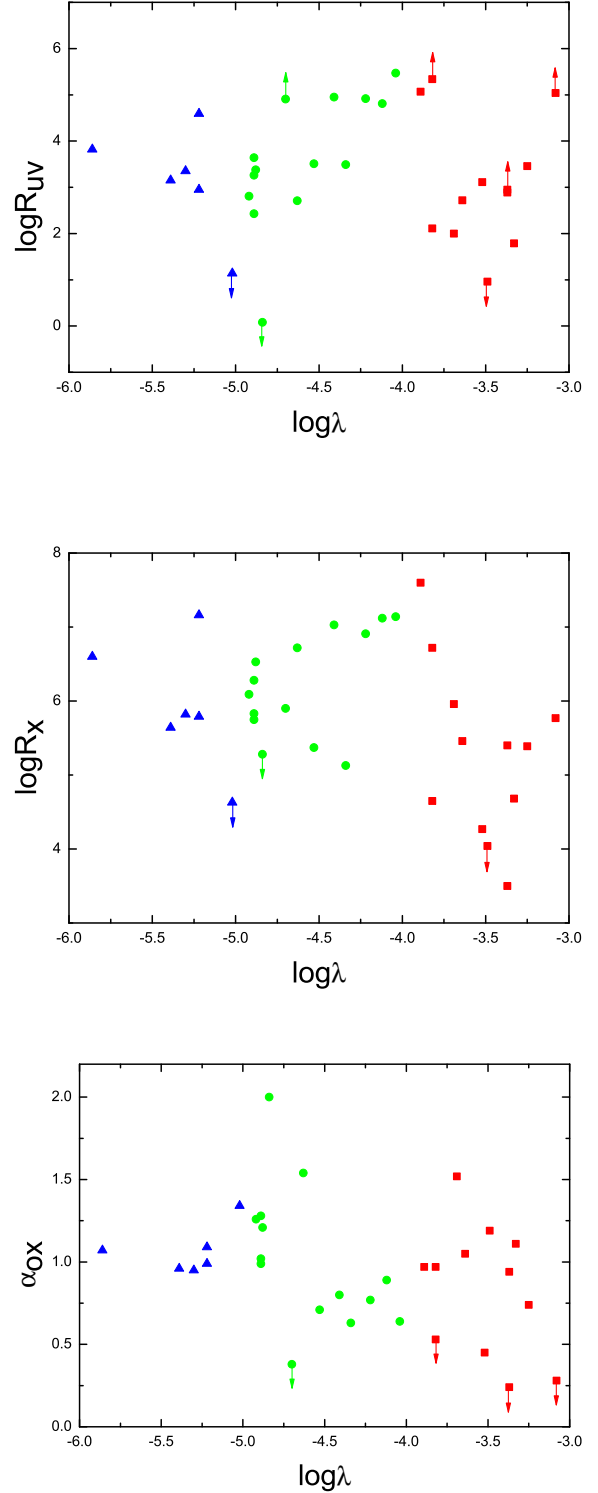


Figure 1. Radio loudnesses (R_{UV} : Top panel; R_X : Middle panel) and optical/UV-to-X-ray spectral index α_{ox} (bottom panel), respectively, as a function of the Eddington ratio λ for LLAGNs. The blue triangles, green circles and red squares are, respectively, for sources whose Eddington ratio is in the range of $-6 < \log \lambda < -5$, $-5 < \log \lambda < -4$, and $-4 < \log \lambda < -3$.

¹ website: <http://ned.ipac.caltech.edu/>

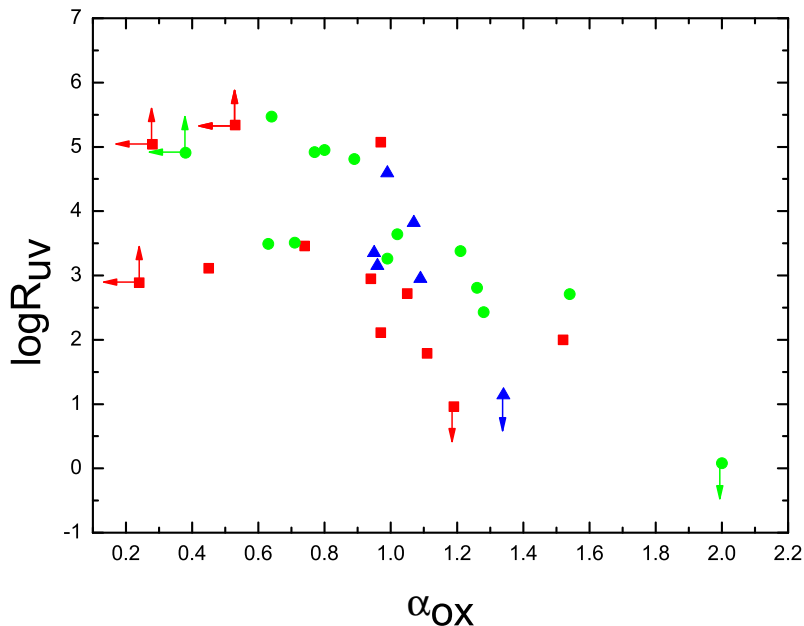


Figure 2. Radio loudnesses R_{UV} as a function of the optical/UV to X-ray spectral index α_{ox} for LLAGNs. The symbols are the same to those in Fig. 1.

therein)², as LLAGNs are systematically louder in radio compared with bright AGNs.

The bottom panel of Fig. 1 shows the relationship between optical/UV-to-X-ray spectral index α_{ox} and Eddington ratio λ . A negative correlation can be derived, i.e. from linear fitting it reads,

$$\alpha_{ox} = (-0.19 \pm 0.09) \log \lambda + 0.12 \pm 0.37. \quad (3)$$

The confidence level of this result is high, 96.8 %. This result is consistent with that given in Xu (2011), where the correlation slope is reported to be -0.16 .

3.2 the $R_{UV}-\alpha_{ox}$ relationship in LLAGNs

We now investigate the relationship between radio-loudness and optical/UV-to-X-ray spectral property. As shown in Fig. 2, it is evident that there is a negative correlation between R_{UV} and α_{ox} for all the three luminosity regimes. The confidence level of correlation analysis for the three regimes are, respectively, 95.4 % (the $-4 < \log \lambda < -3$ regime), 99.9 % (the $-5 < \log \lambda < -4$ regime) and 95.3 % (the $-6 < \log \lambda < -5$ regime). For the whole sample, the confidence level of a negative correlation is larger than 99.9 %, remarkably strong. A linear fit (R_{UV} in logarithmic space) to the data shows that,

$$\log R_{UV} = (-2.39 \pm 0.48) \alpha_{ox} + 5.61 \pm 0.49 \quad (4)$$

For comparison, we show in Fig. 3 the relationship between R_{UV} and α_{ox} for a limited sample of bright AGNs, i.e. Seyfert galaxies with $\lambda > 10^{-2}$. These sources, mainly gathered from Xu (2011), are listed in Table 2. From this figure we find that the

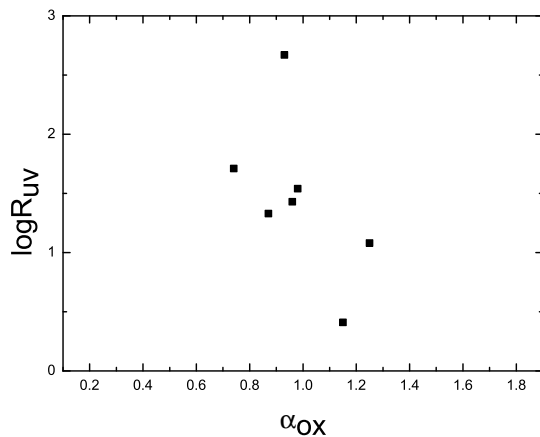


Figure 3. The relationship between radio loudness R_{UV} and the optical/UV to X-ray spectral index α_{ox} for bright AGNs with $\lambda > 10^{-2}$.

correlation between R_{UV} and α_{ox} in bright AGNs (or at least bright Seyferts) is absent/weak, at the confidence level 80.3 %. We note that this bright AGN sample is obviously incomplete; there are numerous bright AGNs exist in literature. However, since in this work we intend to focus on LLAGNs only, the expansion of bright AGNs will be devoted to a separate work.

4 THEORETICAL INTERPRETATION BASED ON TRUNCATED ACCRETION–JET MODEL

It has been known for years that, in LLAGNs systems, there exist negative correlations between radio-loudness R_{UV} and Eddington ratio λ (or UV/X-ray Eddington ratios. See e.g., Maoz 2007; Ho 2008. Admittedly the LLAGN sample in this work provides a null correlation but with large uncertainties, cf. Eq. 1.), and between optical-to-X-ray spectral index α_{ox} and Eddington ratio λ (Xu

² Note that a rough estimation of the LLAGN sample of Ho (2008), which has a larger dynamical range in λ (~ 8 orders of magnitude), indicates $\log R_X \sim -0.8 \log \lambda + const.$. But this steep correlation may be contaminated by AGNs at bright end. When limited to sources with $10^{-6} < \lambda < 10^{-3}$, the slope becomes shallower (see their Fig. 10, and also Fig. 3 in Sikora et al. 2007).

2011). We in this work, report a new negative correlation, i.e. the $R_{UV}-\alpha_{OX}$ correlation, which is likely insensitive to the Eddington ratio. We emphasize that all the three correlations witness large scatter, i.e., for a given λ , both R_{UV} and α_{OX} vary significantly from one source to the other.

We in this Section will try to understand the three correlations as well as their scatter under the truncated accretion–jet model, a model that has been successfully applied to LLAGNs (for review see Yuan & Narayan 2014), e.g., to understand their broadband spectra and also the “fundamental plane” of BH activity. The accretion–jet model utilizes three components (for details, cf. Esin et al. 1997; Yuan & Narayan 2014), i.e. an outer cold SSD, which is truncated at certain radius, an inner hot accretion flow within that radius, and a conical jet near the central black hole. In this work, we argue that the scatters themselves in the three correlations provide additional information on the fundamental properties of accretion flows. Before detailed theoretical analysis, we first speculate that the relativistic beaming effect is not the dominated reason for the scatter in radio-loudness. This is mainly because we exclude in our sample sources with small-viewing-angles, such as Blazars. If the jet is viewed at moderately large (and similar in value) viewing angles, then the difference in the beaming enhancement should be small among different sources (Chen 2017). Consequently, the scatter in radio emission (or R_{UV}) is mainly intrinsic.

We emphasize that, if R_{UV} and α_{OX} depend solely on the accretion rate (or equivalently the luminosity λ), i.e. $R_{UV} \propto \lambda^{-\xi_1}$ and $\alpha_{OX} \propto \lambda^{-\xi_2}$ (here $\xi_1 > 0, \xi_2 > 0$), then their negative correlations will result in a positive $R_{UV}-\alpha_{OX}$ relationship, i.e. $R_{UV} \propto \alpha_{OX}^{\xi_1/\xi_2}$, contradict to what we observed. Even for the weak positive $R_{UV}-\lambda$ correlation reported from our sample, the correlation coefficients $\xi_1 = -0.04$ and $\xi_2 = 0.46$ will lead to a weak relationship, i.e., $R_{UV} \propto \alpha_{OX}^{-0.09}$, inconsistent with the steep one shown in Eq. 4 (see also Fig. 2). It is thus clear that the observed strong negative $R_{UV}-\alpha_{OX}$ correlation should be caused by other factors. Our key idea to this problem, as well as the scatter observed, is to consider the effect of viscosity parameter α .

4.1 basic properties of truncated accretion–jet model

According to hot accretion flow theory (Narayan & Yi 1994; Yuan & Narayan 2014), larger α will lead to higher radial infalling velocity V_R , as $V_R \sim -\alpha C_s^2/\Omega_K$, where C_s is the sound speed (insensitive to \dot{m} when radiative cooling is dynamically unimportant, the case explored in this work.) and Ω_K is the Keplerian rotational velocity (Yuan & Narayan 2014). Consequently the density n and the surface density Σ of the accretion flow will be lower, i.e. $n \propto \dot{m}/\alpha$ and $\Sigma \propto \dot{m}/\alpha$. Hot accretion flow is optically thin, with synchrotron, bremsstrahlung, and the Compton scattering as its major radiation mechanisms (Narayan & Yi 1995). The bolometric luminosity can then be given as,

$$L_{bol} \sim \left(\frac{\dot{m}}{\alpha}\right)^a, \quad (5)$$

where the index a is estimated to be, $a \approx 2$, based on detailed numerical calculations of hot accretion flows (Esin et al. 1997; Merloni et al. 2003; Xie & Yuan 2012).

For LLAGNs, there are two competing components for the emission at optical/UV wavebands. One component is the thermal emission from the outer truncated SSD, which peaks in optical or UV bands, depending on the location of truncated radius. The other component is the Compton scattering of synchrotron emission from the inner hot accretion flow (Manmoto et al. 1997;

Yuan & Narayan 2014). Since our sample is limited to sources whose $\lambda < 10^{-3}$, we argue that the emission at 2500 Å mainly comes from the inner hot accretion flow³. Interestingly, for hot accretion flows around supermassive BHs (the LLAGN case), the optical/UV emission usually is the first Compton up-scattered bump (Manmoto et al. 1997; Yuan & Narayan 2014). The emission from such process has a positive correlation with \dot{m} , as \dot{m} will determine mainly the optical depth (surface density), a quantity that controls the probability of Compton scattering (Sunyaev & Titarchuk 1980; Dermer, Liang & Canfield 1991). On the other hand, the first Compton bump is even more sensitive to the energy of electrons (a.k.a. the electron temperature), as it determines the location (in wavebands) of the peak. For a given \dot{m} , larger α means lower density, or equivalently lower radiative cooling to the electrons. Consequently, the electrons will be more energetic with higher temperatures (Xie & Yuan 2012). The dependence of emission at optical/UV band on parameter α relies on detailed numerical calculations, where Manmoto et al. (1997) reported that the emission at 2500 Å has a positive correlation with α . With the above reasons, we simply write L_{UV} as,

$$L_{UV} \sim (\dot{m}\alpha)^b, \quad (6)$$

where $b \sim 2$. The estimation of b comes from the fact that, the first-order Compton scattering (responsible for the optical/UV emission) depends on the product of the seed photon flux (synchrotron emission, $\propto \dot{m}^{0.5-1}$, cf. Mahadevan 1997; Yuan et al. 2015, note that electron temperature also depends on \dot{m} for the expression in Mahadevan 1997.) and optical depth in vertical direction ($\propto \dot{m}^{1-2}$).

The X-ray emission mainly comes from the high-order (second or even higher) Compton scattering processes in hot accretion flow, which is obviously more sensitive to the optical depth (Sunyaev & Titarchuk 1980; Dermer, Liang & Canfield 1991), compared to the first-order Compton bump (e.g., L_{UV}). With the assumption that the optical depth is relatively small in hot accretion flows, we may write it as,

$$L_X \propto L_{UV} \alpha^{-2} \Sigma^c \\ \propto \dot{m}^{b+1} \alpha^{b-3}, \quad (7)$$

where the index $c \approx 1-2$. Because we exclude moderately bright LLAGNs (whose $10^{-3} < \lambda < 10^{-2}$) from our sample, we may safely assume $c \approx 1$ in the second expression. In the above expression, the factor α^{-2} is introduced to take into account the shift of photon energy (in $h\nu$) of both synchrotron emission and consequently the first Compton bump, as viscosity parameter α changes (cf. Manmoto et al. 1997 for numerical calculations). We also note that, from statistical point of view, the integrated (in 2–10 keV energy band) X-ray luminosity of LLAGNs can roughly be expressed as $L_X(2-10 \text{ keV}) \approx f_X L_{bol}$, where observationally the correction factor f_X is estimated to be $f_X \approx 1/30$ (Gu & Cao 2009; Xu 2011) or $f_X \approx 1/16$ (Ho 2008).

Now we come to estimate the self-absorbed synchrotron radio emission, whose $\alpha_r \approx 0$, from the jet. Based on conical “disc–jet” model, the jet is formed by extracting the rotation energy of the underlying disc. Moreover, the composition of the disc–jet is assumed to be dominated by normal plasma, i.e. electrons and ions, coming from the underlying hot accretion flow. The flat-spectrum

³ Obviously, for brighter systems, i.e. those with $10^{-3} \lesssim \lambda \lesssim 10^{-2}$, the truncated radius is small enough that the emission from the outer SSD should be taken into account.

radio emission (at e.g., 5 GHz) has a power-law dependence on the mass loss rate into the jet \dot{m}_{jet} (Heinz & Sunyaev 2003; Ghisellini et al. 2014), i.e., we have,

$$\begin{aligned} L_R &\propto \dot{m}_{jet}^{1.4} \\ &\propto \dot{m}^{1.4}, \end{aligned} \quad (8)$$

where in the latter expression we assume $\dot{m}_{jet} \propto \dot{m}$. Note that detailed modelling on observations implies a slightly weaker dependence on \dot{m} (e.g., Yuan & Cui 2005; Xie & Yuan 2016). When this correction is taken into account, we would observe slightly steeper correlations between R_{UV} and λ , and R_X and λ , while there is no impact to α_{ox} , see below.

Therefore, the radio loudnesses R_{UV} and R_X can be expressed as,

$$R_{UV} = \frac{L_R}{L_{UV}} \propto \dot{m}^{1.4-b} \alpha^{-b} \propto (\dot{m}/\alpha)^{1.4-b} \alpha^{1.4-2b}, \quad (9)$$

$$R_X = \frac{L_R}{L_X} \propto \dot{m}^{0.4-b} \alpha^{3-b} \propto (\dot{m}/\alpha)^{0.4-b} \alpha^{3.4-2b}. \quad (10)$$

The optical-to-X-ray spectral index α_{ox} can be written as,

$$\alpha_{ox} = 0.384 \log(L_{UV}/L_X) \approx -0.4 \log(\dot{m}/\alpha) + 0.8 \log \alpha + const. \quad (11)$$

4.2 theoretical interpretation on three correlations and their scatters

We now apply the above results to understand the three correlations observed. If we assume that LLAGNs on average have a mean value of α , $\bar{\alpha}$. Then substitute Eq. 5 to Eqs. 9–11, we have,

$$\begin{aligned} \log R_{UV} &\approx -\frac{(b-1.4)}{a} \log L_{bol} - (2b-1.4) \log \bar{\alpha} + const. \\ &\approx -0.3 \log \lambda - 2.6 \log \bar{\alpha} + const., \end{aligned} \quad (12)$$

$$\begin{aligned} \log R_X &\approx -\frac{(b-0.4)}{a} \log L_{bol} - (2b-3.4) \log \bar{\alpha} + const. \\ &\approx -0.8 \log \lambda - 0.6 \log \bar{\alpha} + const., \end{aligned} \quad (13)$$

$$\begin{aligned} \alpha_{ox} &\approx -(0.4/a) \log L_{bol} + 0.8 \log \bar{\alpha} + const. \\ &\approx -0.2 \log \lambda + 0.8 \log \bar{\alpha} + const. \end{aligned} \quad (14)$$

For all the second expressions, we take $a \approx 2$ and $b \approx 2$.

Obviously, based on the truncated accretion–jet scenario, we have naturally reproduced negative correlations between R_{UV} and λ (Eq. 12, for observational results see Sec. 3 and Maoz 2007, Sikora et al. 2007), R_X and λ (Eq. 13, for observational results see Sec. 3 and Ho 2008), and α_{ox} and λ (Eq. 14, for observational results see Sec. 3 and Xu 2011). How to understand the null relationship between R_{UV} and λ reported in this work (but inconsistent with earlier works)? From Eq. 12, we argue it is likely because that R_{UV} – λ correlation is relatively weak (with a slope of -0.3) compared to the large scatter introduced by α (with a slope of -2.6). Interestingly, as noted before in footnote 2, the R_{UV}/R_X – λ correlations will be shallower when we limit to sources with $10^{-6} \leq \lambda \leq 10^{-3}$ (Fig. 3 in Sikora et al. 2007 and Fig. 10 in Ho 2008). The correlation slope derived from the whole AGN sample may be contaminated by those brighter end AGNs. The scatter observed in the three correlations, on the other hand, could be considered as the deviations of α of individual sources to the mean value $\bar{\alpha}$. We note that Xu (2011) had already reported a negative α_{ox} – λ correlation together with detailed numerical calculations of hot accretion flow.

There are two points in our theoretical interpretation that worth further emphasis. The first is that, the R_X – λ correlation is

steeper than the R_{UV} – λ correlation. The second is that, R_X – λ correlation has a much weaker dependence on α , compared to the R_{UV} – λ correlation. Combining these two reasons, we expect that, if α varies from source to source, then the R_{UV} – λ relationship will have larger scatter.

Then, what determines the value of α in accretion flows? According to recent advanced MHD simulations (Bai & Stone 2013; Salvesen et al. 2016), the value of “effective” α varies from 0.01 to 1, depending on the net vertical magnetic flux and/or magnetic field configuration carried by the accreted material. Interestingly, such large difference in α will produce a scatter of 5.2 orders of magnitude in R_{UV} (cf. Eq. 12), which is in rough agreement with the ~ 6 -order-of-magnitude scatter in our sample, cf. the top panel of Fig. 1.

Finally we examine the R_{UV} – α_{ox} relationship. With substitution of λ in Eqs. 12 & 14, one may quickly find a positive correlation between R_{UV} and α_{ox} . We note that this is actually misleading, as it only reflects the dependence on bolometric luminosity L_{bol} . Considering the large scatters in both R_{UV} and α_{ox} , the impact of λ on the R_{UV} versus α_{ox} is insignificant, e.g., the different symbols in Fig. 2 overlaps with one another. This actually inspires us to consider other factors, where we attribute to the viscosity parameter α . Since R_{UV} has a negative correlation with α , while α_{ox} has a positive relationship with α (cf. Eqs. 12 & 14), we expect to have a negative correlation between R_{UV} and α_{ox} . Eliminating α in Eqs. 12 & 14, we have,

$$\log R_{UV} \approx -3.25 \alpha_{ox} - 0.95 \log \lambda + const., \quad (15)$$

where $b \approx 2$ is adopted. Obviously, a strong negative R_{UV} – α_{ox} correlation is reproduced. The slope agrees with the observed value (-2.39 ± 0.48 , cf. Eq. 4) at 2σ level. However, we admit that the moderate strong dependence on λ predicted by this simple theoretical model disagrees with observations.

5 SUMMARY

In this work, we gather from literature a sample of LLAGNs whose X-rays are likely from the emission of hot accretion flows. The luminosity range of this sample is $10^{-6} \lesssim \lambda \lesssim 10^{-3}$, i.e. we exclude from our sample sources whose X-rays are likely dominated by emission from jet, and also moderately bright LLAGNs whose UV emission may have contributions from outer SSD. Our LLAGN sample includes 32 sources, among which 14 sources are low- λ Seyfert galaxies and the rest 18 sources are LINERs. From this sample, we observe a strong negative correlation between R_{UV} and α_{ox} (cf. Eq. 4), and this correlation is insensitive to the Eddington ratio λ .

Then, based on the truncated accretion–jet model, we provide comprehensive understanding to this new observation, together with the other two negative correlations reported in literature, i.e. R_X – λ and α_{ox} – λ correlations (note that we produce a null R_{UV} – λ relationship with large uncertainty). The scatter in these correlations derived is argued to relate to the viscosity parameter α of the hot accretion flow component.

From theoretical point of view, viscosity parameter determines the critical luminosity of hot accretion flow, above which it will enter into the “physically-bright AGN” accretion mode (Xie & Yuan 2012; Qiao et al. 2013; Yuan & Narayan 2014). More importantly, it is argued based on MHD simulations that, α has a strong dependence on the net vertical magnetic flux and/or magnetic field configuration carried by the accreted material (e.g.,

Hawley et al. 1995; Backman et al. 2008; Bai & Stone 2013; Salvesen et al. 2016). For example, the value of α can vary about two order of magnitudes ($\sim 0.01 - 1$) when the magnetic field strength β (the ratio of gas to magnetic pressure) varies from 10^5 to 10 (Bai & Stone 2013; Salvesen et al. 2016). In this sense, deeper understanding on the correlation as well as the scatter of the $R_{UV}-\alpha_{ox}$ relationship will hopefully reveal the strength and/or configuration of magnetic field in hot accretion flows, which will also help to constrain the launching mechanism of jet (see e.g., Blandford & Payne 1982; Hawley et al. 2015). Detailed numerical calculations are devoted to our future work.

ACKNOWLEDGEMENTS

We appreciate the referee for valuable comments, and Minfeng Gu for useful discussions. We are supported in part by the National Program on Key Research and Development Project of China (Grant Nos. 2016YFA0400804 and 2016YFA0400704), the Youth Innovation Promotion Association of Chinese Academy of Sciences (CAS) (ids. 2015216 and 2016243), the Natural Science Foundation of China (grants 11373056, 11233006, 11573051, 11633006 and 11661161012), the Natural Science Foundation of Shanghai (grant 17ZR1435800), the Key Research Program of Frontier Sciences of CAS (No. QYZDJ-SSW-SYS008). This work has made extensive use of the NASA/IPAC Extragalactic Database (NED), which is operated by the Jet Propulsion Laboratory, California Institute of Technology, under contract with the National Aeronautics and Space Administration (NASA).

REFERENCES

- Belloni T. M., 2010, in “The Jet Paradigm - From Microquasars to Quasars”, ed. T. Belloni, Lecture Notes in Physics, Springer-Verlag, Berlin, 794, 53
- Backman, E. G., Penna, R. F., Varniere, P., 2008, *New Astro.*, 13, 244
- Bai, X. N., Stone, J. M., 2013, *ApJ*, 767, 30
- Blandford, R. D., & Begelman, M. C. 1999, *MNRAS*, 303, L1
- Blandford, R. D., & Payne, D. G. 1982, *MNRAS*, 199, 883
- Blandford R. D., Königl A., 1979, *ApJ*, 232, 34
- Bu D. F., Yuan F., Wu M., Cuadra J., 2013, *MNRAS*, 434, 1692
- Bu D. F., Yuan F., Gan Z. M., Yang X. H., 2016, *ApJ*, 818, 83
- Cao X., & Wang J.-X., 2014, *MNRAS*, 444, 20
- Carrillo, R., Masegosa, J., Dultzin-Hacyan, D., & Ordoñez, R. 1999, *RevMexAA*, 35, 187
- Chen, Liang, 2017, *ApJ*, arXiv:1706.04611
- Connolly, S., McHardy, I., Skipper, C., Emmanoulopoulos, D., 2016, *MNRAS*, 459, 3963
- Dermer C. D., Liang E. P., Canfield E., 1991, *ApJ*, 369, 410
- Done, C., 2014, in *Suzaku-MAXI 2014: Expanding the Frontiers of the X-ray Universe*, proceedings of a conference held 19-22 February, 2014 at Ehime University, Japan. Eds. M. Ishida, R. Petre, and K. Mitsuda., p.300
- Done, C., Gierliński, M., & Kubota, A. 2007, *A&A Rev.*, 15, 1
- Esin, A. A., McClintock, J. E., & Narayan, R. 1997, *ApJ*, 489, 865
- Ghisellini G., Tavecchio F., Maraschi L., Celotti A., Sbaratto T., 2014, *Nature*, 515, 376
- Greene J. E., Ho L. C., Ulvestad J. S., 2006, *ApJ*, 636, 56
- Gu, M., & Cao, X. 2009, *MNRAS*, 399, 349
- Hawley J. F., Fendt C., Hardcastle M., Nokhrina E., Tchekhovskoy A., 2015, *Spac. Sci. Rev.*, 191, 441
- Hawley J. F., Gammie C. F., Balbus S. A., 1995, *ApJ*, 440, 742
- Heinz S., Sunyaev R. A., 2003, *MNRAS*, 343, L59
- Hernández-García L., González-Martín O., Marquez I., Masegosa J., 2013, *A&A*, 556, 47
- Ho, L. C. 2008, *ARA&A*, 46, 475
- Ho L. C., 2009, *ApJ*, 699, 626
- Ho L. C., Filippenko A. V., Sargent W. L. W., 1997a, *ApJS*, 112, 315
- Ho, L. C., Filippenko, A. V., Sargent, W. L. W., & Peng, C. Y. 1997b, *ApJS*, 112, 391
- Lasota, J.-P., Abramowicz, M. A., Chen, X., et al. 1996, *ApJ*, 462, 142
- Mahadevan, R., 1997, *ApJ*, 477, 585
- Manmoto, T., Mineshige, S., & Kusunose, M. 1997, *ApJ*, 489, 791
- Maoz, D. 2007, *MNRAS*, 377, 1696
- Maoz D., Nagar N. M., Falcke H., Wilson A. S., 2005, *ApJ*, 625, 699
- Merloni A., Heinz S., di Matteo T., 2003, *MNRAS*, 345, 1057
- Narayan, R., & Yi, I. 1994, *ApJ*, 428, L13
- Narayan, R., & Yi, I. 1995, *ApJ*, 452, 710
- Nemmen, R. S., Storchi-Bergmann, T., Eracleous, M., & Yuan, F. 2010, in *IAU Symp. 267, Co-Evolution of Central Black Holes and Galaxies*, ed. B. M. Peterson, R. S. Somerville, & T. Storchi-Bergmann (Cambridge: Cambridge Univ. Press), 313
- Nemmen R. S., Storchi-Bergmann T., Eracleous M., 2014, *MNRAS*, 438, 2804
- Qiao E., Liu B. F., Panessa F., Liu J. Y., 2013, *ApJ*, 777, 102
- Sadowski A., Narayan R., Tchekhovskoy A., Abarca D., Zhu Y., McKinney J. C., 2015, *MNRAS*, 447, 49
- Salvesen G., Simon J. B., Armitage P. J., & Begelman M. C., 2016, *MNRAS*, 457, 857
- Shakura, N. I., & Sunyaev, R. A. 1973, *A&A*, 24, 337
- Shang Z. et al., 2005, *ApJ*, 619, 41
- Sikora M., Stawarz Ł., Lasota J.-P., 2007, *ApJ*, 658, 815
- Sobolewska, M. A., Siemiginowska, A., & Gierliński, M. 2011, *MNRAS*, 413, 2259
- Sunyaev R. A., Titarchuk L. G., 1980, *A&A*, 86, 121
- Ulvestad, J. S., Ho, L. C., 2001. *ApJ*, 562, L133
- Ward, M., Elvis, M., Fabbiano, G., et al. 1987, *ApJ*, 315, 74
- Wu, Q., Yuan, F., & Cao, X. 2007, *ApJ*, 669, 96
- Xie F. G., Yuan F., 2012, *MNRAS*, 427, 1580
- Xie F. G., Yuan F., 2016, *MNRAS*, 456, 4377
- Xie F. G., Yuan F., 2017, *ApJ*, 836, 104
- Xie F. G., Zdziarski A. A., Ma R., Yang Q. X., 2016, *MNRAS*, 463, 2287
- Xu, Y.-D., 2011, *ApJ*, 739, 64
- Yang Q. X., Xie F. G., Yuan F., Zdziarski A. A., Gierliński M., Ho L. C., Yu Z., 2015, *MNRAS*, 447, 1692
- Younes G., Porquet D., Sabra B., Reeves J. N., 2011, *A&A*, 530, 149
- Yu Z., Yuan F., Ho L. C., 2011, *ApJ*, 726, 87
- Yuan, F., & Cui, W. 2005, *ApJ*, 629, 408
- Yuan F., Gan Z., Narayan R., Sadowski A., Bu D., Bai X. N., 2015, *ApJ*, 804, 101
- Yuan F., & Narayan R., 2014, *ARA&A*, 52, 529
- Yuan F., Quataert E., Narayan R. 2003, *ApJ* 598, 301
- Yuan F., Wu M., Bu D., 2012, *ApJ*, 761, 129
- Yuan F., Yu Z., Ho L. C., 2009, *ApJ*, 703, 1034